†Electronic Supporting Information

Crystallophore: a versatile lanthanide complex for protein crystallography combining nucleating effect, phasing properties and luminescence.

Sylvain Engilberge,[a] François Riobé,[b] Sebastiano Di Pietro,[b] Louise Lassalle,[a] Nicolas Coquelle,[a] Charles-Adrien Arnaud,[a] Delphine Pitrat,[b] Jean-Christophe Mulatier,[b] Dominique Madern,[a] Cécile Breyton,[a] Olivier Maury,[b]* and Eric Girard.[a]*

a. Institut de Biologie Structurale (IBS), Univ Grenoble Alpes, CEA, CNRS, 38044 Grenoble, France. E-mail: eric.girard@ibs.fr

b. Univ Lyon, Ens de Lyon, CNRS UMR 5182, Université Claude Bernard Lyon 1, Laboratoire de Chimie, F-69342 Lyon, France. E-mail: olivier.maury@ens-lyon.fr

Content:

Tb-Xo4 synthesis.

Starting reagents were purchased from Sigma-Aldrich or Acros and used without further purification. All organic solvents were dried on molecular sieve for 48h. The complex Tb-Xo4 is now commercially available by Molecular Dimensions under the name *Crystallophore N°1*.

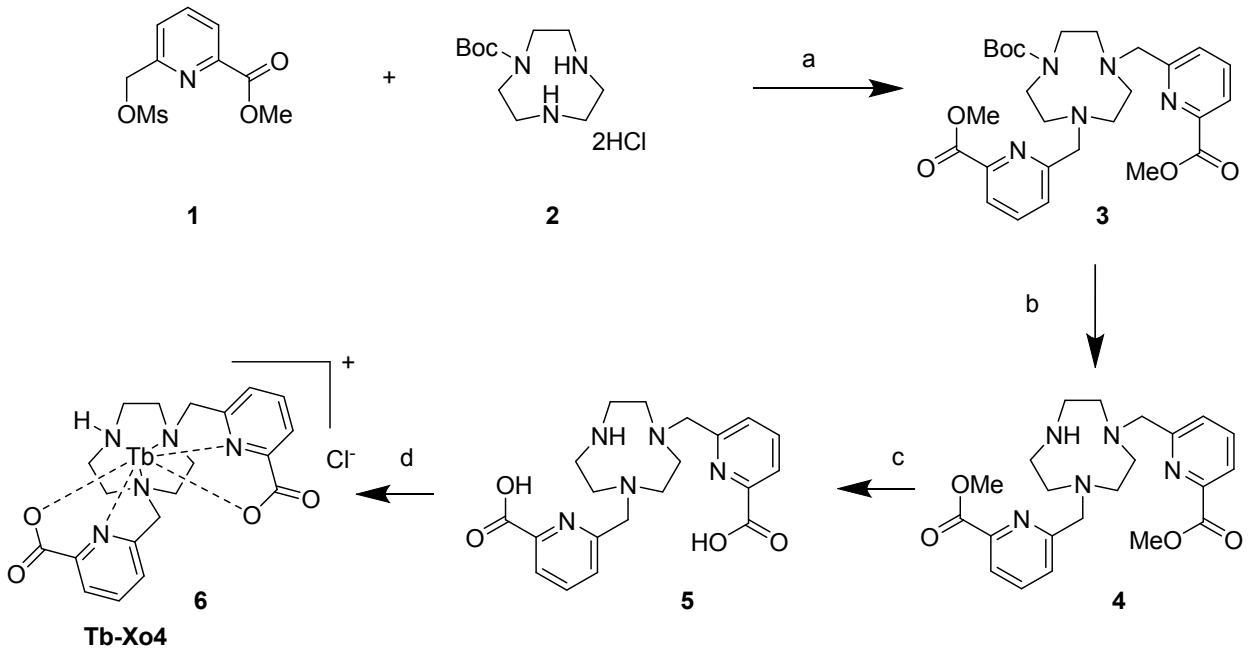

Scheme S1. Synthesis of Tb-Xo4

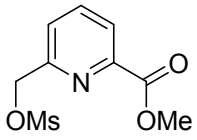

Synthesis of compound **1**. 2-methanesulfonyloxymethyl-6-methoxycarbonyl-pyridine was prepared according to the procedure previously reported.[1]

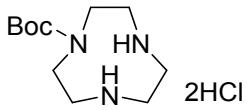

Synthesis of compound **2**. The synthesis was done by the previously reported procedure.[2]

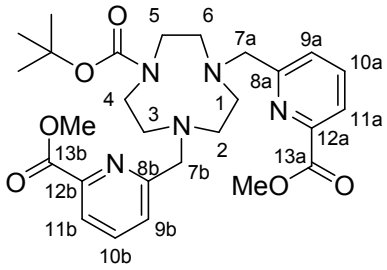

Synthesis of compound **3**. 360 mg of compound **2** (1.19 mmol) and 760 mg of sodium carbonate (7.15 mmol, 6 eq.) were dried under reduced pressure in a schlenk and dissolved in 100 mL of acetonitrile. Under argon, 710 mg of compound **1** (2.74 mmol, 2.3 eq.) were added to the suspension before heating 12h at 70°C. At room temperature, the mixture was filtered on a fritted glass and concentrated under reduce pressure. Crude product was the purified on alumina (activity III, eluent DCM then DCM/MeOH 96/4 v/v) to obtained 532 mg of compound **3** (1.01mmol, yield: 85%), as a yellow oil.

^{1}H NMR (500 MHz, $CDCl_3$) δ 7.99 (dd, J = 6 Hz, 2H, H11), 7.86 – 7.65 (m, 4H, H9), 3.98 (s, 10H, H7+OMe), 3.39 (d, J = 30 Hz, 4H, H4H5), 3.11 (s, 2H, H3H6), 2.95 (s, 2H, H3'H6'), 2.66 (d, J = 31 Hz, 4H, H1H2), 1.44 (s, 9H, Boc).

^{13}C NMR (126 MHz, $CDCl_3$) δ 166.01, 166.09 (C13), 161.43, 161.60 (C8), 155.88(CO(Boc)) 147.45(C12), 137.42 (d,C10), (s), 126.19,126.46 (C9), 123.70 (C11), 79.48 (C(Boc)), 63.70 (d, C7), 57.21 (C1C2), 55.37 (s), 55.11 (s), 54.67 (s), 53.04 (OMe), 50.54, 49.95 (C4C5), 28.72 (CH3(Boc)).

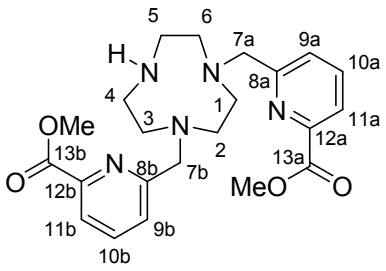

Synthesis of compound **4**. In 100mL of DCM, 5 mL of trifluoroacetic acid were added to a solution of 427 mg of the compound **3** (0.81 mmol). After stirring for 5h at RT, the mixture was evaporated removing the excess of TFA thank to several additions of toluene. Crude product was purified on alumina (activity III, DCM/MeOH (MeOH 1 to 7% v/v). 315 mg of a yellowish solid were obtained (0.74 mmol, yield: 90%).

^{1}H NMR (500 MHz, $CDCl_3$) δ 7.96 (dd, *J* = 7.7, 0.5 Hz, 2H, H11), 7.71 (t, *J* = 8 Hz, 2H, H10), 7.42 (dd, *J* = 7.9, 0.5 Hz, 2H), 3.98 (d, 10H, H7+OMe), 3.40 (t, *J* = 5 Hz, 4H, H4H5), 3.03 (t, *J* = 5 Hz, 4H, H3H6), 2.71 (s, 4H, H1H2).

^{13}C NMR (126 MHz, $CDCl_3$) δ 165.37 (C13), 159.43 (C8), 147.59 (C12), 137.87 (C10), 126.10 (C9), 124.02 (C11), 60.95 (C7), 54.60 (C1C2), 53.31 (OMe), 51.66 (C3C6), 46.52 (C4C5).

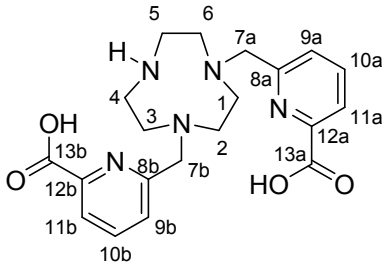

Synthesis of compound **5**. The compound **5** was formed *in situ* from 110 mg of diester **4** (0.26 mmol) in presence of NaOH (2 eq.) in a 20 mL mixture MeOH/H_2O (1/1, v/v) stirred for 3h at 50°C, before the complexation step.

^{1}H NMR (500 MHz, D_2O) δ 7.77 (d, J = 7.1 Hz, 2H, H9), 7.69 (t, J = 7.7 Hz, 2H, H10), 7.29 (d, J = 7.2 Hz, 2H, H11), 3.86 (s, 4H, H7), 3.08 (t, J = 5.9 Hz, 4H, H4H5), 2.91 (t, J = 5.9 Hz, 4H, H3H6), 2.65 (s, 4H, H1H2).

^{13}C NMR (126 MHz, MeOD/D_2O) δ 173.22 (C13), 158.44 (C8), 153.01 (C12), 138.23 (C10), 125.17 (C11), 122.40 (C9), 60.27 (C7), 50.53 (C1,C2), 47.12 (C3,C6), 44.10 (C4,C5).

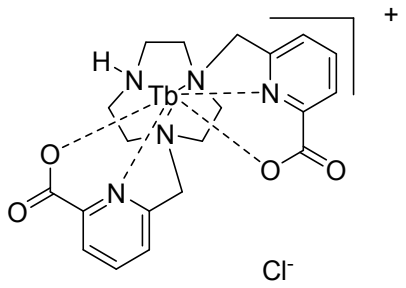

Synthesis of compound **6, TbXo4**. The crude ligand **5** formed *in situ* in a 20 mL mixture MeOH/H_2O (1/1, v/v) was neutralized adding HCl (1M). Then, 96 mg of $TbCl_3$,$6H_2O$ (0.26 mmol, 1 eq.) were added and the mixture was stirred overnight at 50°C. After evaporation, the crude product is solubilized in 5mL of MeOH and filtered over a fritted glass. Then, the mixture is purified by size exclusion chromatography (Sephadex®, LH20, eluent: water) to obtain 114 mg of a colorless powder (0.19 mmol, yield: 75%).

^{1}H-NMR (300 MHz, D_2O) δ 129.027, 76.025, 72.666, 67.478, 45.868, 39.225, 24.001, 8.512, 0.086, -7.811, -16.846, -19.040, -29.499, -35.303, -45.253, -53.748, -82.665, -92.662, -127.747.

HR-MS (ESI-TOF) calculated M+: 556.1003; measured: 556.0990

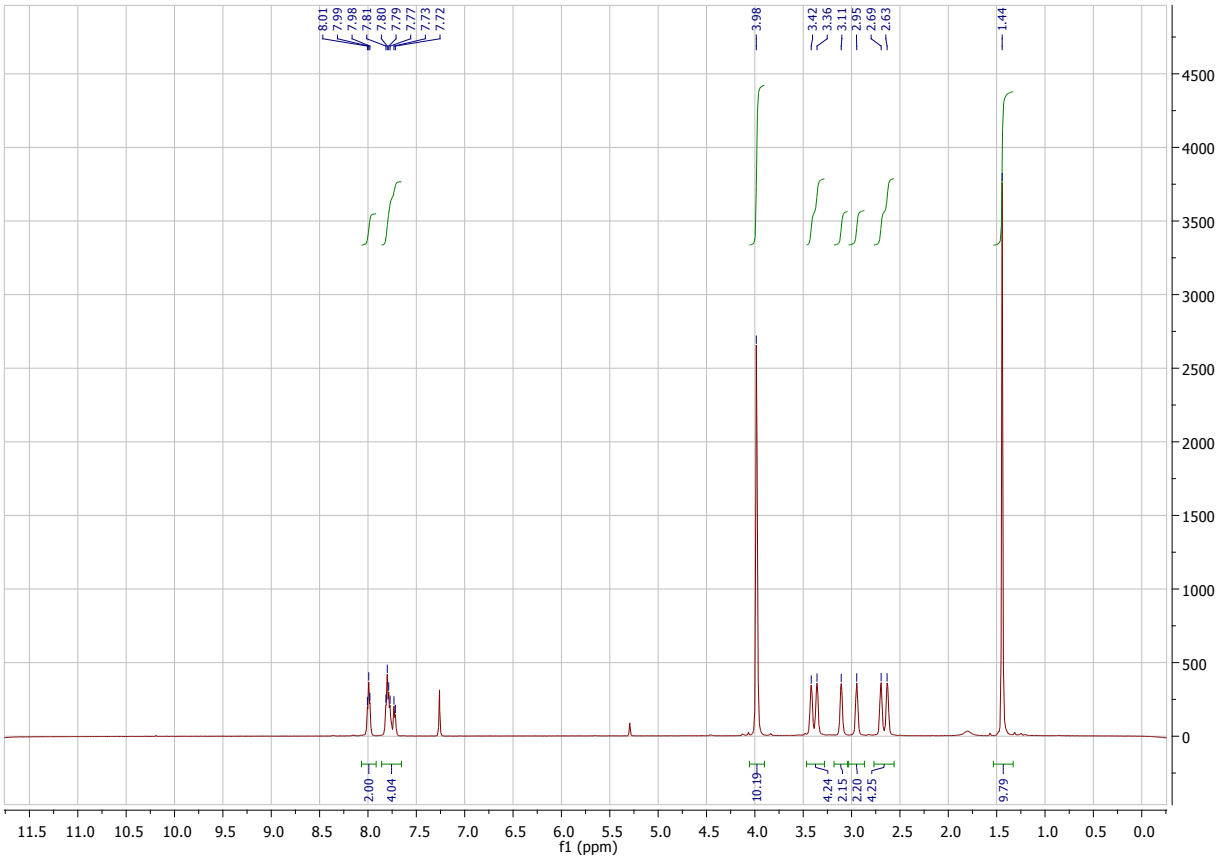

Figure S1. ^{1}H-NMR of compound **3**.

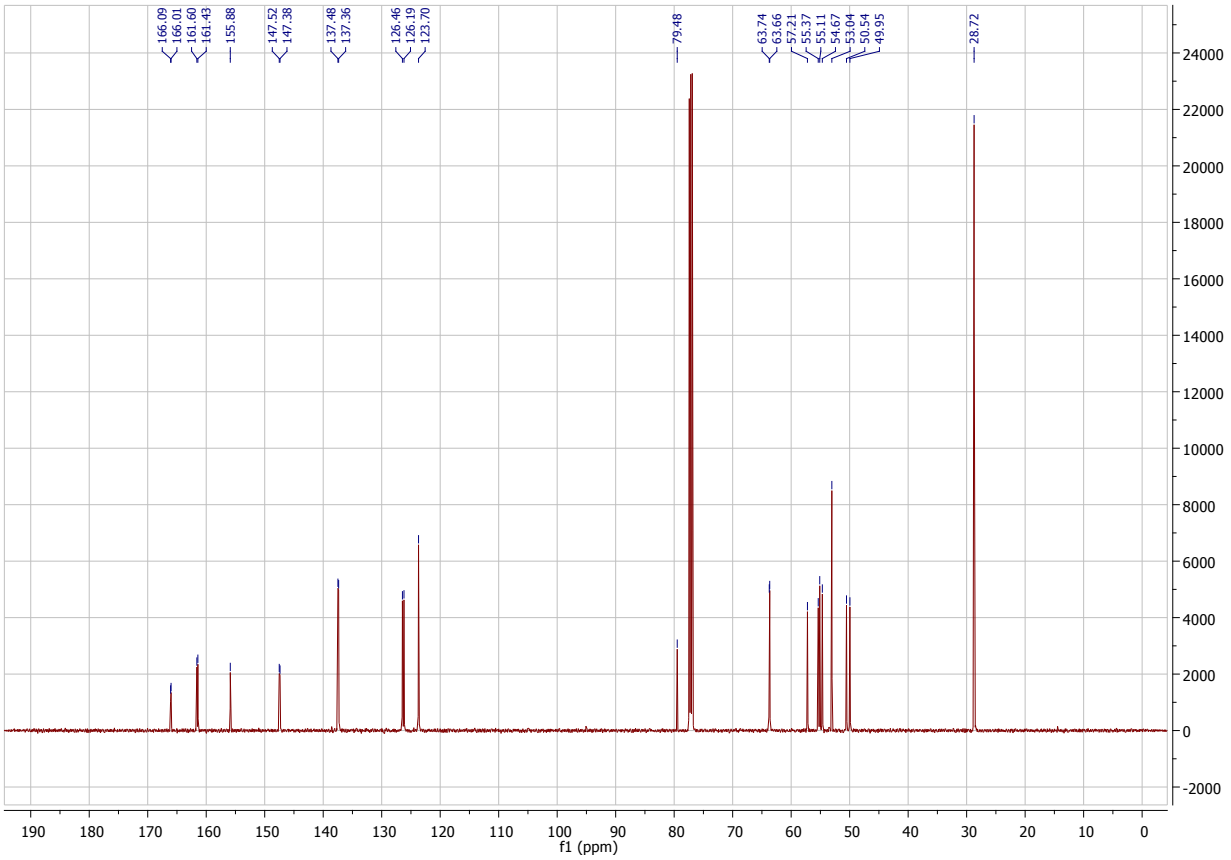

Figure S2. ^{13}C-NMR of compound **3**.

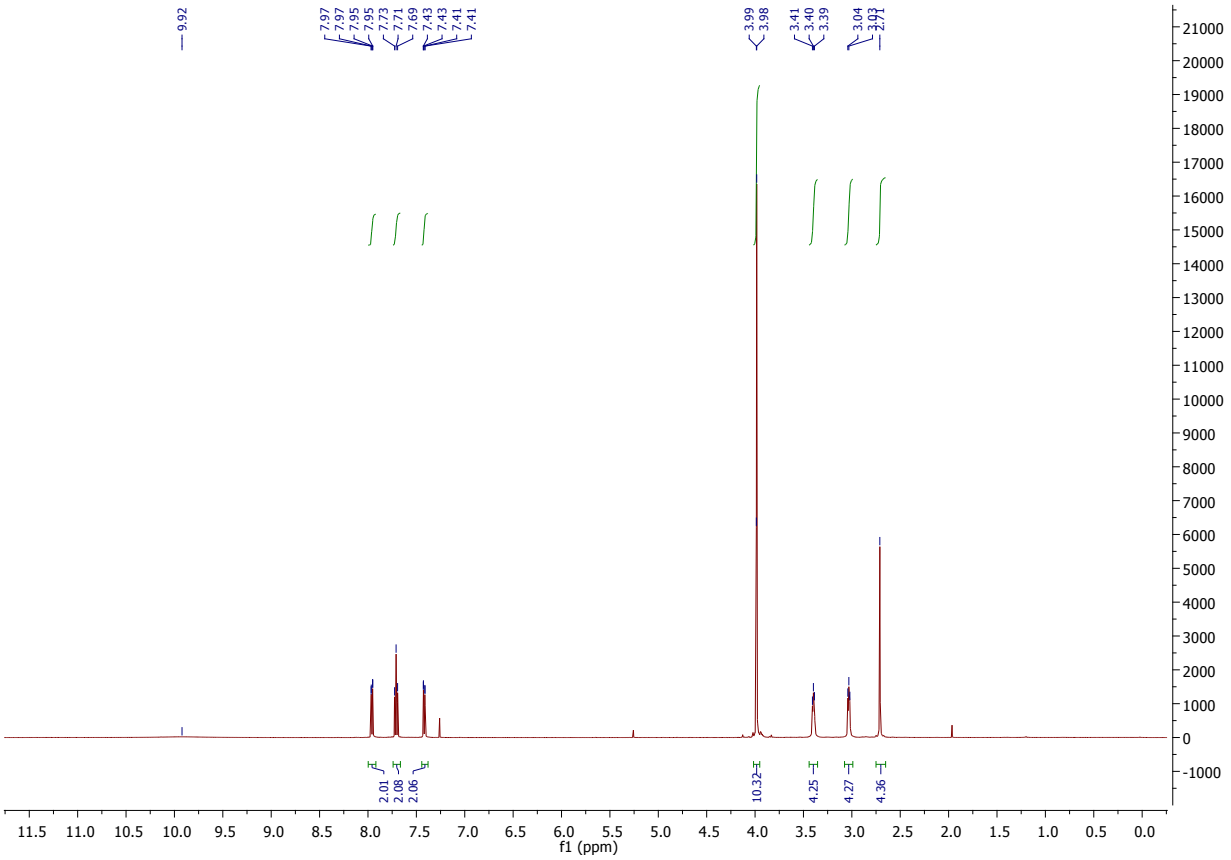

Figure S3. ^{1}H-NMR of compound **4**.

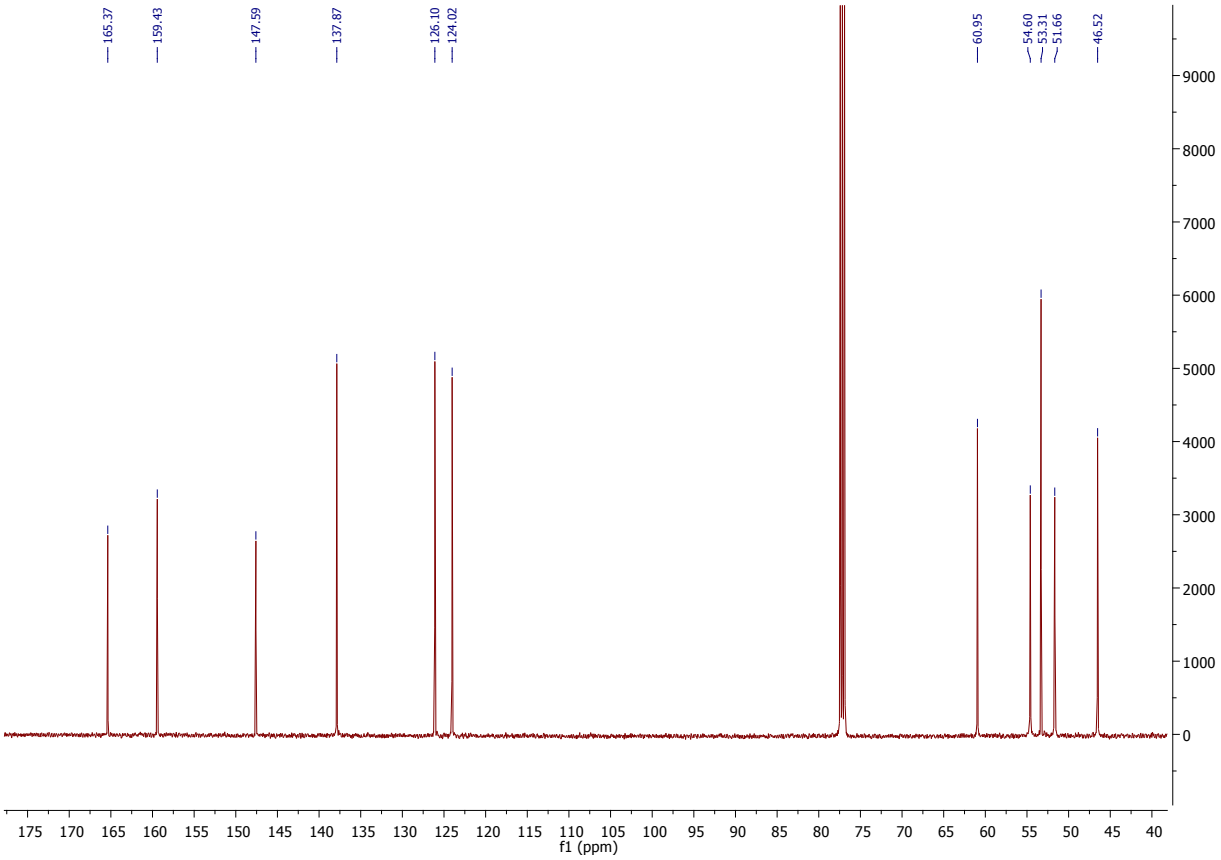

Figure S4. ^{13}C-NMR of compound **4**.

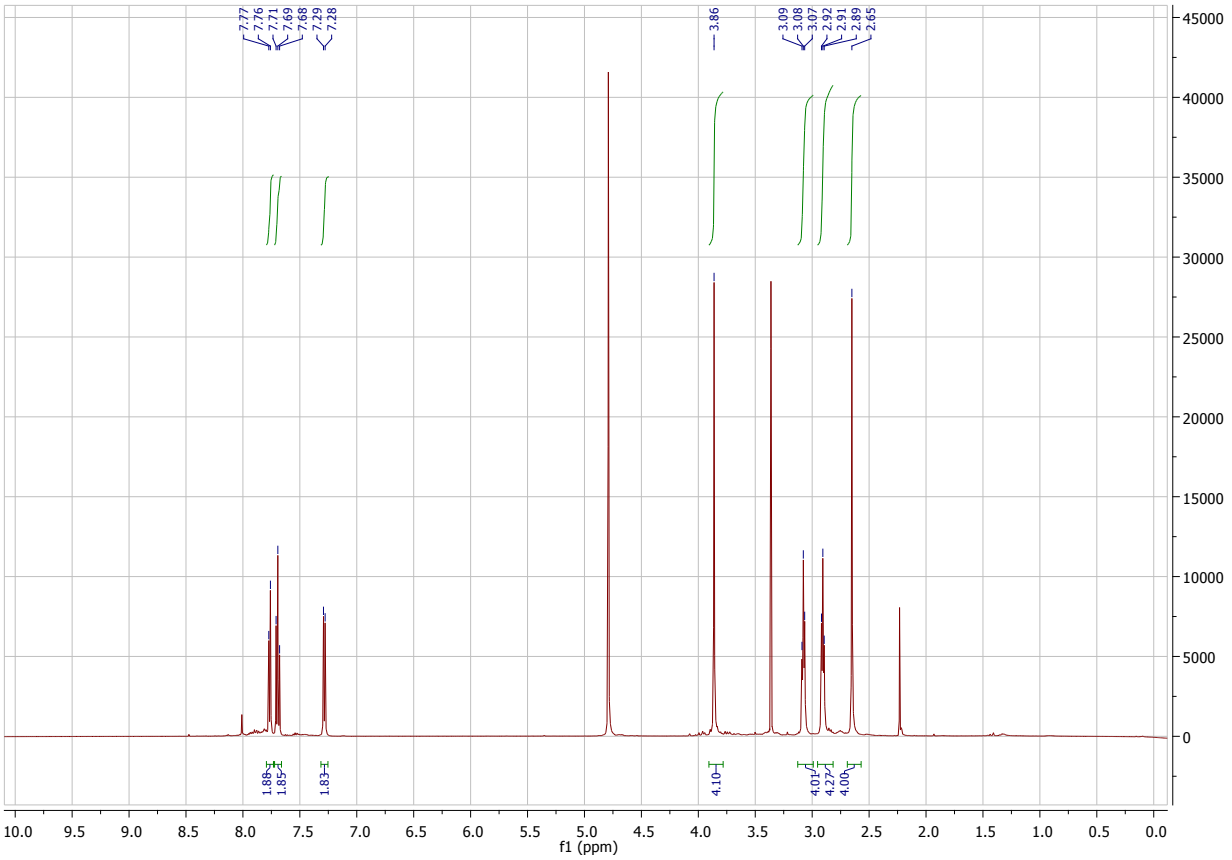

Figure S5. ^{1}H-NMR of compound **5**.

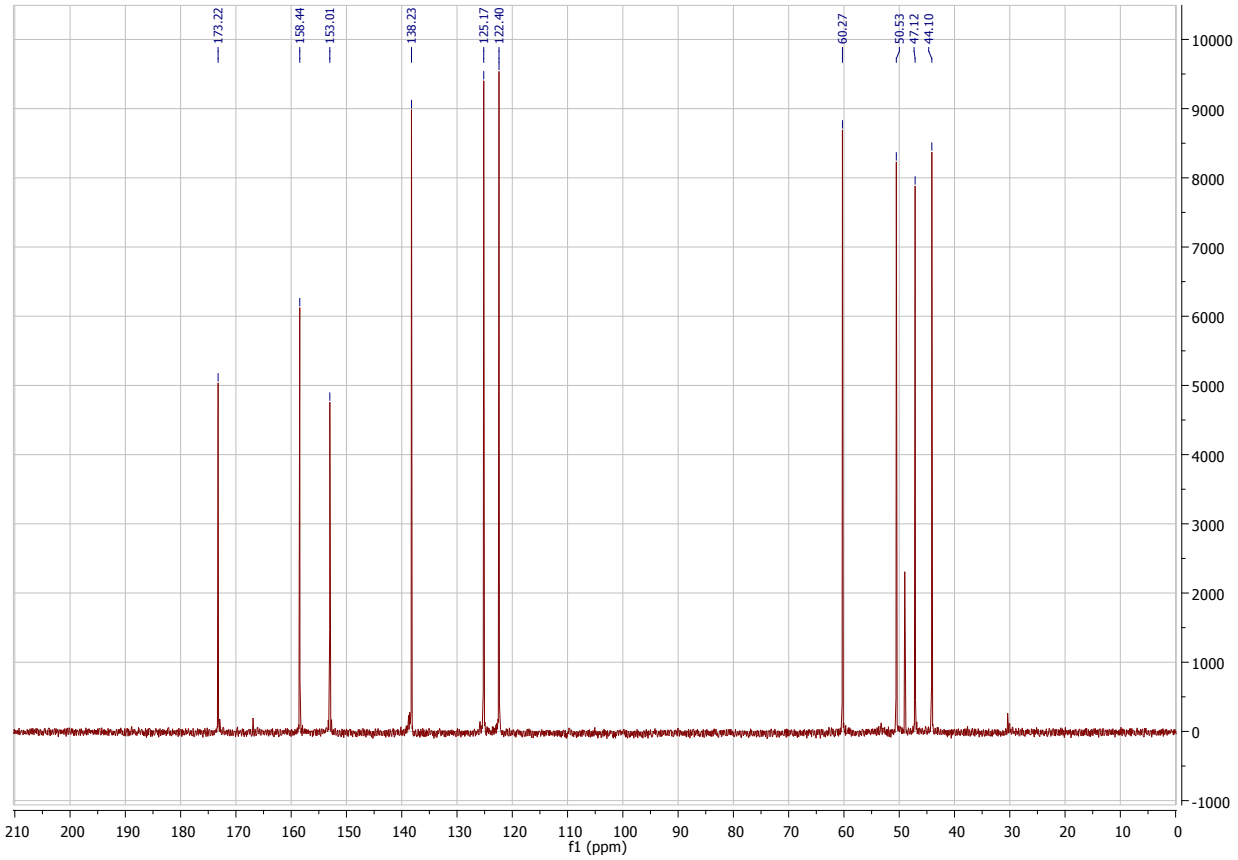

Figure S6. ^{13}C-NMR of compound **5**.

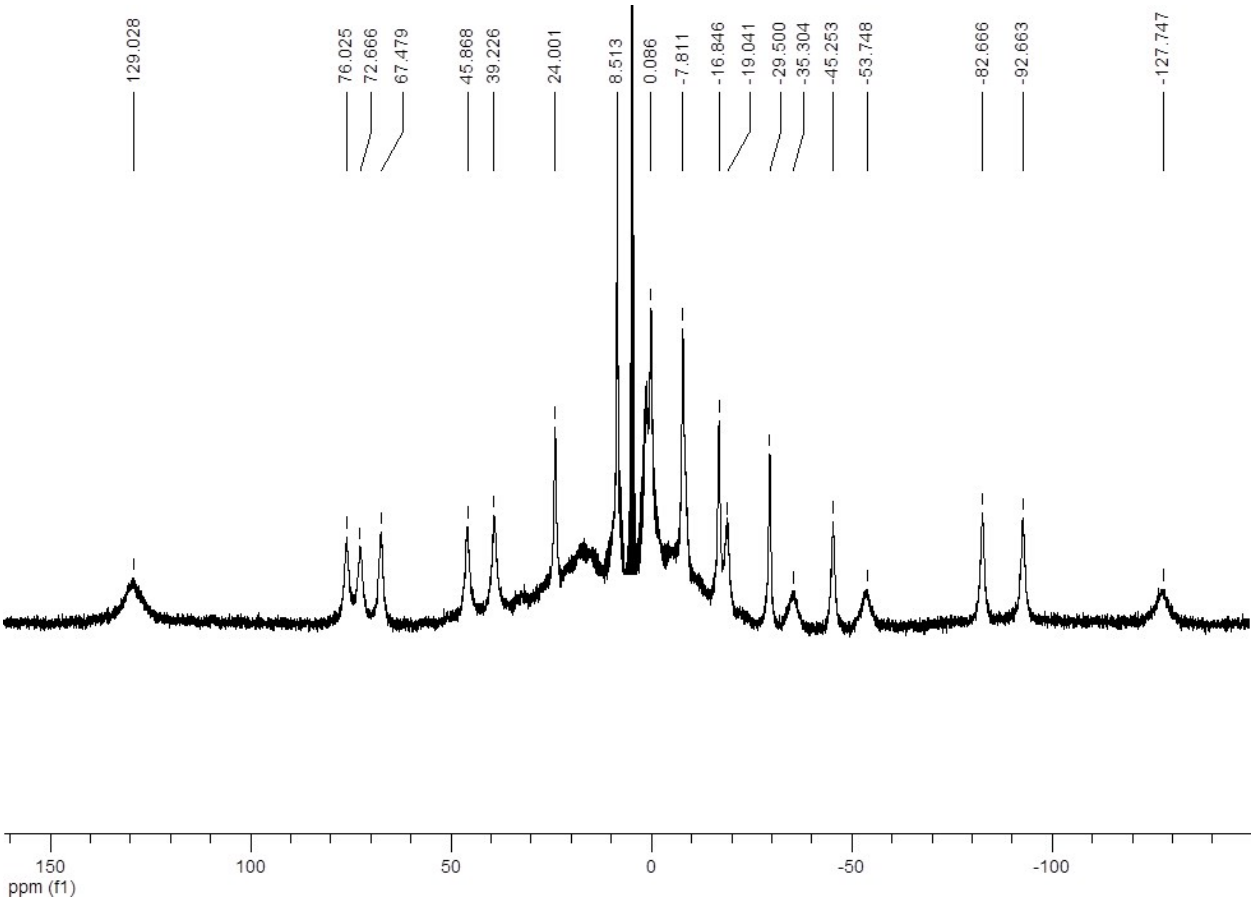

Figure S7. ^{1}H-NMR of compound **6**.

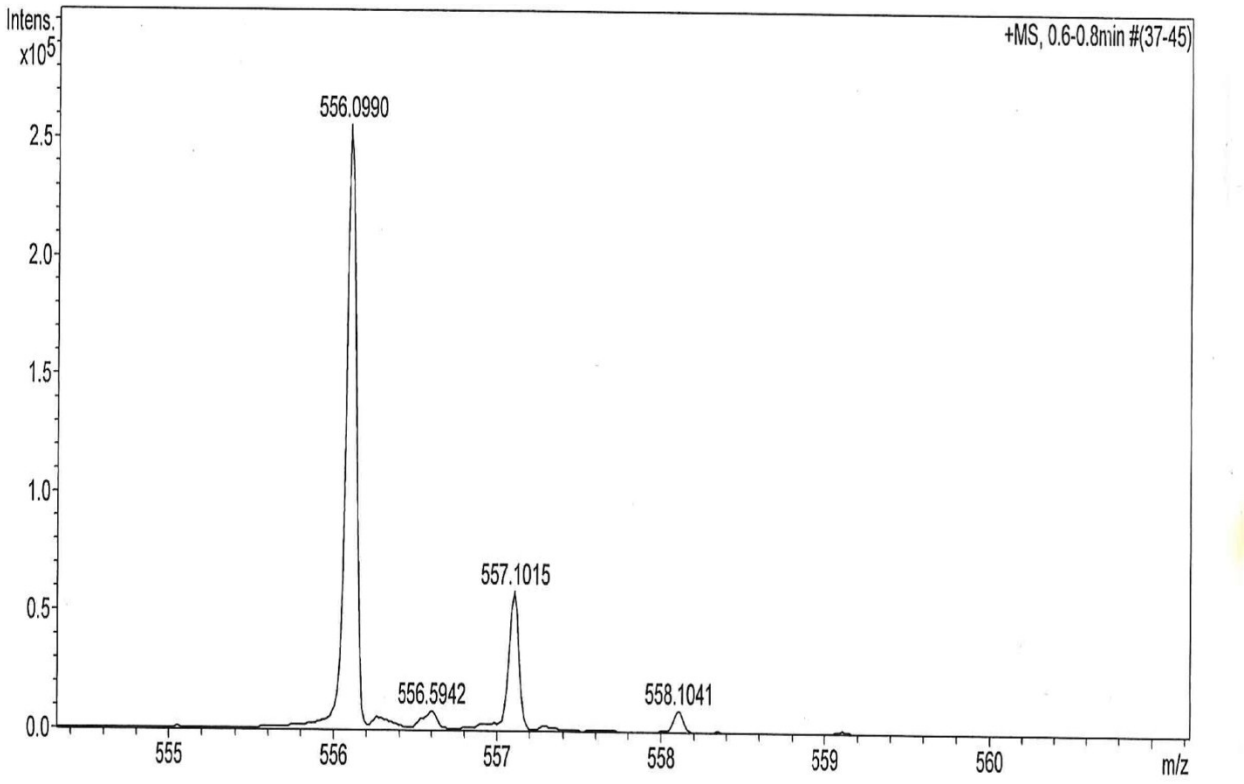

Figure S8. HR-MS (ESI-TOF) of compound **6**.

Protein set.

Eight proteins were used for the reported study (Table S1); six of them were of known structure (HEWL, thaumatin, proteinase K, pb9, protease1 and glyoxylate/hydroxypyruvate reductase (GRHPR)) and the remaining two were of unknown structure (MDH , pb6).

The commercial proteins (lysozyme from hen egg white; Roche catalogue N° 10837059001, Thaumatin from *T. Danielli*; Sigma catalogue N° T7638 and proteinase K; Roche catalogue N° 03115879001) were prepared at 20 mg/ml in deionized water, without any further purification. The other protein targets were purified in the laboratory. Protease 1 from *Pyrococcus horikhoshii* (PhP1) was expressed and purified as mentioned in X Du *et al.* [3] to a final concentration of 10 mg/ml in 20 mM Tris pH 7.5 and 150 mM NaCl. pb9 was purified as described in A Flayhan *et al.* .[4] pb6 was purified using the same protocol. Both were concentrated to 10 mg/ml in 20 mM

Tris pH 8. PfGRHPR from *Pyrococcus furiosus* was expressed and purified according to Lassalle *et al.* .[5] The protein solution was stocked at 10 mg/ml in 20 mM Tris pH 7.5 and 150mM NaCl. MDH is a halophilic protein purified using the protocol described in Madern *et al.* .[6] The final concentration was 10 mg/ml in 20 mM Tris pH 7.5 and 1.5 M KCl.

Table S1. Proteins indications

Protein	Organism	Molecular weight (Da)	Biological unit
HEWL	*Gallus gallus*	14313	Monomer
Proteinase K	*E. album*	28934	Monomer
Thaumatin	*T. daniellii*	22132	Monomer
Protease1	*P. horikoshii*	18624	Hexamer
GRHPR	*P. furiosus*	38342	Monomer
pb9	T5 phage	24452	Monomer
pb6	T5 phage	50413	Monomer
MDH	Synthetic	32547	Tetramer

Automated crystallization.

Prior to automated crystallization experiments, the lanthanide complex Tb-Xo4 is directly dissolved with the protein solution. Briefly, a given amount of Tb-Xo4 is weighted in an Eppendorff tube. The tube is shortly spin down to pellet the powder. Then, the pellet is re-suspended with the appropriate volume of protein solution to reach a final Tb-Xo4 concentration of 10 mM (*e.g.* 100 µl of protein for 0.581 mg of Tb-Xo4). The solution is centrifuged at 10000 rpm for 5 minutes to remove any aggregates. The solution is immediately used for crystallization.

All automated screening trials were done at the High-Throughput Crystallization Laboratory (HTXlab) platform (EMBL Grenoble). The crystallization experiments were performed with a Cartesian PixSys 4200 crystallization robot (Genomic Solutions, U.K.) and set up by mixing 100 nL of protein solution with 100 nL of precipitant solution in CrystalQuick™ (Greiner Bio-one) or CrystalDirect™ (MiTeGen) plates with a reservoir solution of 80 and 45 µL, respectively.

Storage (at 293K) and imaging of the plates was ensured by a RockImager system (Formulatrix, Inc., U.S.). Each crystallization trial was performed in parallel with and without Tb-Xo4 (10 mM). We selected the 6 standard screens proposed by the HTXlab for initial screening, for a total of 576 conditions. During the time of this study, HTXlab has modified its screens formulation. Depending on the protein, different screens were thus used as listed in Table S2.

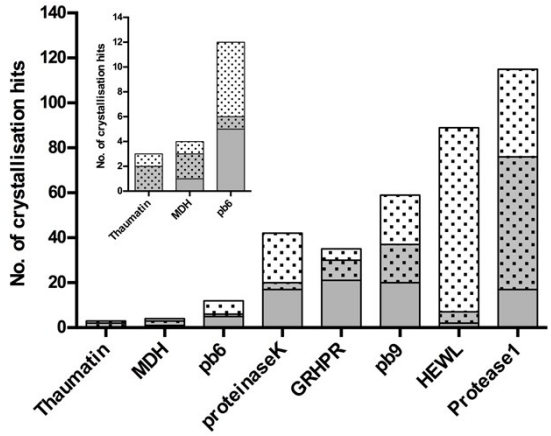

Figure S9. Evaluation of Tb-Xo4 nucleating properties. Details of the results of automated crystallization screening (576 conditions) performed on the 8 proteins tested. The number of crystallization hits is depicted in grey for native protein and with dots for protein supplemented with 10 mM Tb-Xo4. As a result, the shared conditions are represented in grey with dots. Observation after 7 days.

Table S2. Crystallization screening used

Proteins	**HEWL - Thaumatin - Proteinase K - pb9 - GRHPR - Protease 1**	
Screen 1	Qiagen/Nextal	The Classics Suite
Screen 2	Molecular Dimensions	JCSG+
Screen 3	Molecular Dimensions	PACT premier
Screen 4	Qiagen/Nextal	PEGs-I
Screen 5	Hampton Research	Grid Screen Salt
Screen 6	Rigaku Reagents	Wizard I & II
Proteins	**MDH - pb6**	
Screen 1	Hampton Research	Crystal Screen Lite ; PEG/Ion
Screen 2	Hampton Research	Natrix and MembFac
Screen 3	Hampton Research	Grid Screen Sodium Malonate ; Grid Screen Ammonium Sulfate ; Quik Screen ; Home-made screen with sodium formate from HTXlab platform (Salt Grid *)
Screen 4	Hampton Research	Grid Screen PEG-LiCl ; Grid Screen PEG 6K ; Grid Screen MPD Home-made screen with with PEG 5000 MME from HTXlab platform (Polymer Grid *)
Screen 5	Hampton Research	Index
Screen 6	Qiagen/Nextal	The Classics Suite

* https://embl.fr/htxlab/index.php?option=com_content&view=article&id=38&Itemid=172

Crystallization diagram determination.

Crystallization diagrams were determined using HEWL, pb9 and pb6, by testing the impact of precipitant and protein concentrations in presence and absence of Tb-Xo4. Hanging drops were set up in 24 wells VDX plates with silicon glass cover slides (Hampton research), at 293 K. All the chemicals were purchased from Sigma Aldrich. For each protein, the most promising condition obtained during the automated crystallization screening was based on best crystal morphology observed. In each case, it was the starting point to further explore the crystallization diagram.

HEWL and pb6 were used to evaluate the influence of 10 mM Tb-Xo4 on the crystallization at different protein concentrations (Main text Fig. 2 and Fig. 4a). For that, Tb-Xo4 was prepared as a stock solution in water at 10 mM. Each crystallization drops were prepared by mixing 1.5 µl of

protein solution, 1.5 µl of 10 mM Tb-Xo4 solution and 1.5 µl of precipitant solution. The precipitant compositions are listed in Table S2. All plates were setup in triplicate for 4 protein concentrations 5, 10, 15 and 20 mg/ml with and without 10 mM Tb-Xo4. A crystallization condition is considered successful if a crystal appeared in at least two drops out of three. Diagrams displayed in main text Fig. 4 correspond to plate inspections after 2 days.

HEWL and pb9 were used to determine the optimal Tb-Xo4 concentration for crystallization (Main text Fig.1 and Fig. S10). Stocks solutions of Tb-Xo4 were prepared in water at various concentrations (2.5, 5, 10, 15, 20, 30, 40, 50, 75 and 100 mM). Each crystallization drop was prepared by mixing 1.5 µl of protein solution, 1.5 µl of Tb-Xo4 solution at a given concentration and 1.5 µl of precipitant solution (Table S3). Plates were inspected after two days.

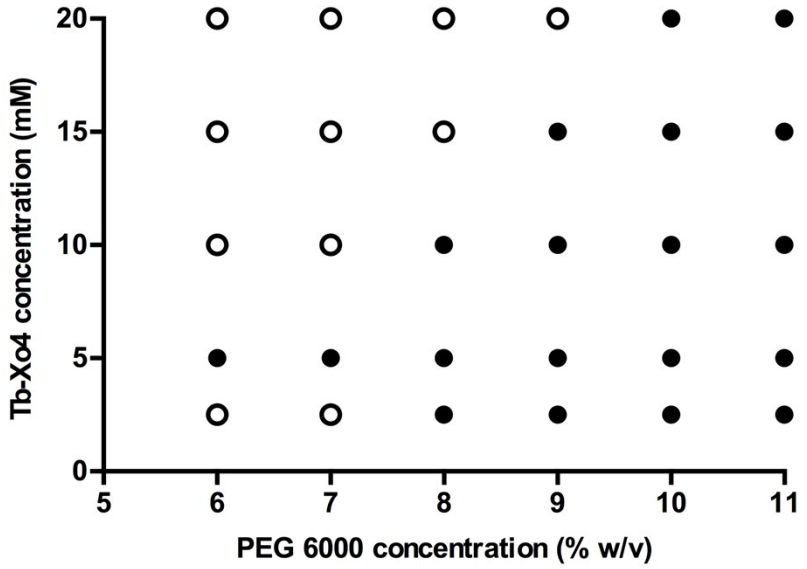

Figure S10. Crystallization diagram of pb9 (10 mg/ml) after two days with different Tb-Xo4 concentrations (2.5 to 100 mM). Black dots represent conditions where crystals are observed. No crystal was observed for Tb-Xo4 concentration above 20 mM.

Luminescence evaluation.

The luminescence spectra (Main text Fig. 7a) was measured using a Horiba-Jobin Yvon Fluorolog-3® spectrofluorimeter, equipped with a three slit double grating excitation and emission monochromator. The steady-state luminescence was excited by unpolarized light from a 450 W xenon CW lamp and detected at a 90° angle by a Hamamatsu R928 photomultiplier

tube.

The luminescence images displayed in Figs. 7b and 7c were acquired using a LEICA Wild M3C binocular and a UV-LED source from Ocean Optics, Model LLS-365, coupled to a 1 mm optical fibre shining on the crystallization drop.

Crystallization conditions used for structure determination.

The conventional crystallization conditions (commercial proteins), as well as unique hits determined through high-throughput screening, used for structure determination, are listed in Table S3. Unique conditions obtained in presence of Tb-Xo4 are indicated in bold. For MDH, pb6 and pb9, among these unique conditions, the best promising hits were manually reproduced, optimized and used for structure determination.

Table S3. Protein crystallization conditions

Protein	Protein concentration (mg/ml)	Crystallization conditions	Cryoprotection #
HEWL	5 to 20	200 to 950 mM sodium chloride in 100 mM sodium acetate buffer pH 4.6	20 % Glycerol
Proteinase K	20	0.9 to 1.4 M ammonium sulfate in cacodylate buffer pH 6.5	20 % Glycerol
Thaumatin	20	0.9 to 1.4 M sodium potassium tartrate and bis tris propane buffer pH 6.5	20 % Glycerol
Protease1	10	1.9 to 2.4 ammonium sulfate and 0.2 M sodium potassium tartrate and 100 mM trisodium citrate dihydrate.	20 % Glycerol
GRHPR	10	14 to 24 % PEG 400 and 100 mM NaCl in 100 mM sodium acetate buffer pH 5.2	20 % PEG 400
pb9	10	**6 to 11 % PEG 6000 and 5 % MPD in 100 mM HEPES buffer pH 7.5**	20 % MPD
pb6	5 to 20	**11 to 16 % PEG 6000 in 100 mM Hepes pH 7.5**	20 % PEG 400
MDH	10	**55 to 65 % MPD in 100 mM MES pH 6.5**	

* Tb-Xo4 unique crystallization condition are highlighted in bold
# % of cryoprotectant added to the crystallization condition

***In situ* data collection and data processing.**

576 screening conditions in MiTeGen CrystalDirect plates were set up in duplicate at the HTX lab with HEWL and pb9, without and with 10 mM Tb-Xo4. After 15 days, the plates were directly submitted to X-ray for *in situ* diffraction with a 6-axis robot goniometer as installed on the BM30A beamline at the European Synchrotron Radiation Facility (ESRF, Grenoble).[7]

In the case of HEWL plates, the beam size was set to 250 x 250 μm^2 and 10 frames with an exposure time of 1 second for an angular sweep of 1° were recorded per hit. To assess diffraction quality of the lysozyme crystals obtained in absence and presence of 10 mM Tb-Xo4, the recently developed program NanoPeakCell [8] was used to: i) select frames containing diffraction information (threshold value of 400) ii) perform background subtraction *via* azimuthal integration, in order to remove as much scattering from the crystallization plate as possible and iii) localize Bragg peaks. To be sure not to consider any remaining scattering from the crystallization plate after background subtraction, contiguous regions of the detector (more than 200 pixels large) above the threshold value used to detect Bragg peaks (40) were masked out. Finally, all Bragg peaks were binned by resolution (10 bins ranging from 50 to 1.4 Å, Fig. 5). The analysis was performed on 20 native drops and 113 Tb-Xo4-containing drops, encompassing 9 drops with common crystallization conditions. Using the criteria described above, NanoPeakCell analysis resulted in the exploitation of 576 images for drops with crystals obtained with only Tb-Xo4, 21 images for drops with native crystals only and 76 (with Tb-Xo4) or 71 (without Tb-Xo4) images for drops with crystals grown in common crystallization conditions. This difference could be explained by an improper centring resulting in loss of diffraction upon plate rotation or radiation damage could impair diffraction quality, resulting in weaker diffraction (if not no diffraction) and some images were not considered as hits in the processing pipeline. Such a semi-automated procedure was also attempted with pb9 diffraction patterns but remained unfruitful, because of poorer diffraction quality.

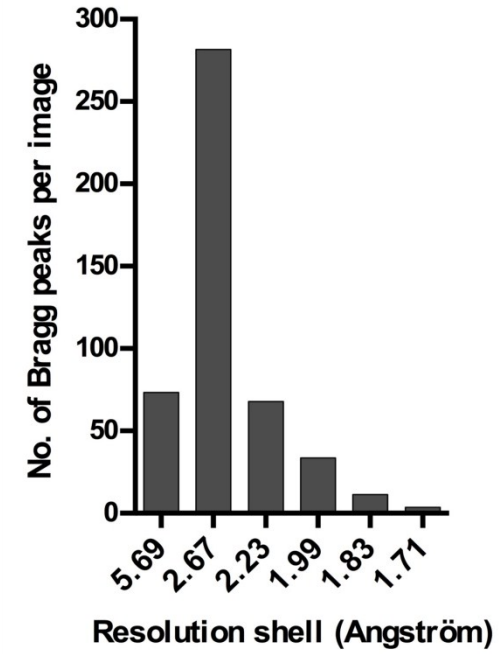

Figure S11. Diffraction quality (measured as the number of Bragg peaks per image) as a function of resolution of crystals corresponding to 104 unique Tb-Xo4 crystallization conditions.

Structure determination.

In order to evaluate the phasing power of Tb-Xo4, anomalous-based data collection were conducted. Prior to data collection, crystals were soaked in their respective mother liquor supplemented with a cryo-protectant as indicated in Table S3. When necessary, the cryo-protective step was also used as a heavy atom soak. In that case, the cryo-protection solution was supplemented with 100 mM Tb-Xo4 with soaking time indicated in Table 1. Crystals were then cryo-cooled in liquid nitrogen. To fully exploit the anomalous contribution of terbium, an X-ray fluorescence scan was systematically performed to precisely determine the peak and the inflection wavelengths of the Tb L_{III} absorption peak and properly set the X-ray energy.

X-ray diffraction data were collected on FIP-BM30A beamline at the European Synchrotron Radiation Facility (ESRF, Grenoble, France) on a single crystal. pb9 data were collected on ID23-1 beamline (ESRF, Grenoble, France). Diffraction frames were integrated using the program XDS [9] and the integrated intensities were scaled and merged using the CCP4 programs SCALA and TRUNCATE respectively.[10] All structures were solved *de novo* by SAD (Single-wavelength Anomalous Diffraction) or MAD (Multiple-wavelengths Anomalous Diffraction) methods (Table 1). The same protocol was applied for all structure determination and consisted

in phasing with AutoSHARP,[11] including determination of anomalous scatterer positions with SHELXD program [12] and phase improvement with SOLOMON,[13] followed by a round of automatic model building with BUCCANEER (CCP4). All softwares were used with standard set-up. Crystallographic software support is provided by SBGrid.[14] Phasing statistics are summarised in Table 1.

pb9 structure refinement.

The model automatically built with BUCCANEER was manually completed and improved in COOT [15] prior to refinement. Refinement was performed with PHENIX [16] using energy minimization and annealing in torsion-angle space in the first round. After this first refinement run, it was possible to model the Xo4 ligand for 3 Tb-Xo4 binding sites out of 15 identified with an anomalous Fourier synthesis. This model was then optimized through iterative cycles of refinement and model building. At the final cycles of the refinement, hydrogens were added (except for ligands and solvent molecules) and TLS refinement was performed, using the TLSMD server to identify the appropriate TLS groups.[17] Data and refinement statistics are summarized in Table S4. The atomic coordinated and measured structure factor amplitudes for pb9 have been deposited in the Protein Data Bank with accession code 5MF2.

Figures were generated using Pymol (www.pymol.org).

Table S4. Data collection and refinement statistics

	pb9
Data collection	
Space group	P 1 2_1 1
Cell dimensions	
a, b, c, Å	71.464 95.502 71.492
α, β, γ, °	90 103.463 90
	Peak
Wavelength, Å	1.6484
Resolution, Å	48.38 - 2.0 (2.07 - 2.00)
R_{merge}	0.094 (1.060)
I / σ(I)	9.50 (1.40)
Completeness, %	98.8 (94.3)
Multiplicity	6.6 (6.0)
Refinement	
Resolution, Å	48.38 - 2.0 (2.07 - 2.0)
No. reflections	62691 (6174)
R_{work} / R_{free}	0.2101 (0.3530) / 0.2355 (0.3523)
No. atoms	6196
Protein	5792
Ligand/ion	106
Water	298
B-factors, Å^2	49.25
Protein	49.10
Ligand/ion	61.20
Water	47.90
R.m.s deviations	
Bond lengths, Å	0.003
Bond angles, °	0.60
Ramachandran	
Favored, %	97.33
Allowed, %	2.11
Outliers, %	0.56

References

1 T. Storr, B. R. Cameron, R. A. Gossage, H. Yee, R. T. Skerlj, M. C. Darkes, S. P. Fricker, G. J. Bridger, N. A. Davies, M. T. Wilson, K. P. Maresca and J. Zubieta, *Eur. J. Inorg. Chem.*, 2005, **2005**, 2685–2697.

2 S. J. Butler, B. K. McMahon, R. Pal, D. Parker and J. W. Walton, *Chemistry*, 2013, **19**, 9511–9517.

3 X. Du, I. G. Choi, R. Kim, W. Wang, J. Jancarik, H. Yokota and S. H. Kim, *Proc Natl Acad Sci USA*, 2000, **97**, 14079–14084.

4 A. Flayhan, F. M. D. Vellieux, R. Lurz, O. Maury, C. Contreras-Martel, E. Girard, P. Boulanger and C. Breyton, *J. Virol.*, 2014, **88**, 820–828.

5 L. Lassalle, S. Engilberge, D. Madern, P. Vauclare, B. Franzetti and E. Girard, *Sci Rep*, 2016, **6**, 20629.

6 D. Madern and C. Ebel, *Biochimie*, 2007, **89**, 981–987.

7 L. Jacquamet, J. Joly, A. Bertoni, P. Charrault, M. Pirocchi, X. Vernede, F. Bouis, F. Borel, J. P. Périn, T. Denis, J. L. Rechatin and J. L. Ferrer, *Journal of synchrotron radiation*, 2009, **16**, 14–21.

8 N. Coquelle, A. S. Brewster, U. Kapp, A. Shilova, B. Weinhausen, M. Burghammer and J.-P. Colletier, *Acta Crystallogr D Biol Crystallogr*, 2015, **71**, 1184–1196.

9 W. Kabsch, *Acta Crystallogr D Biol Crystallogr*, 2010, **66**, 125–132.

10 Collaborative Computational Project Number 4, *Acta Crystallogr D Biol Crystallogr*, 1994, **50**, 760–763.

11 C. Vonrhein, E. Blanc, P. Roversi and G. Bricogne, *Methods Mol. Biol.*, 2007, **364**, 215–230.

12 G. M. Sheldrick, *Acta Crystallogr A Found Crystallogr*, 2008, **64**, 112–122.

13 J. P. Abrahams and A. G. Leslie, *Acta Crystallogr D Biol Crystallogr*, 1996, **52**, 30–42.

14 A. Morin, B. Eisenbraun, J. Key, P. C. Sanschagrin, M. A. Timony, M. Ottaviano and P. Sliz, *Elife*, 2013, **2**, e01456.

15 P. Emsley, B. Lohkamp, W. G. Scott and K. Cowtan, *Acta Crystallogr D Biol Crystallogr*, 2010, **66**, 486–501.

16 P. D. Adams, P. V. Afonine, G. Bunkóczi, V. B. Chen, I. W. Davis, N. Echols, J. J. Headd, L. W. Hung, G. J. Kapral, R. W. Grosse-Kunstleve, A. J. McCoy, N. W. Moriarty, R. Oeffner, R. J. Read, D. C. Richardson, J. S. Richardson, T. C. Terwilliger and P. H. Zwart, *Acta Crystallogr D Biol Crystallogr*, 2010, **66**, 213–221.

17 J. Painter and E. A. Merritt, *Acta Crystallogr D Biol Crystallogr*, 2006, **62**, 439–450.